

Design of Resistive-Loaded Transverse Electromagnetic Horn Antenna for Air-Coupled Ground Penetrating Radar

Youcheng Wang^{1, *} and Xiaojuan Zhang²

Abstract—Design of a resistive-loaded Transverse Electromagnetic (TEM) horn antenna for air-coupled ground penetrating radar (GPR) is proposed in this paper. As the focus is on the application in sensing pavement subsurface, some issues should be considered, such as ultra-bandwidth (UWB) performance, air-coupled detection, high fidelity, compact structure, and simple fabrication. The resistive-loaded horn antenna with a microstrip-type balun was constructed and measured to facilitate the issues. With the radiation towards concrete ground at a height of 0.5 meters, the measured results suggested that the impedance bandwidth of the antenna was 0.5 ~ 14 GHz with a return loss less than -10 dB. The radiation waveform of the horn antenna also showed a late-time ring. A radar experiment result showed that the antenna performed excellently for pavement layer detection.

1. INTRODUCTION

Short duration pulse has been widely applied in Ground Penetrating Radar (GPR) with high resolution. Some types of GPRs have already been developed for subsurface detection, such as sensing pavement subsurface [1–7], vital sign detection [8], and pipe detection [9]. UWB antennas have been researched including Vivaldi antenna [10, 11], bow-tie antenna [12], TEM horn antenna [13–15], quad ridged horn antenna [16], etc. Mostly, GPR antennas are coupled with ground-coupled to achieve deeper detection ranges. Bow-tie antennas, which have ultra-bandwidth and excellent radiation characteristics, have been widely applied in ground-coupled detection. A short impulse excited into the antenna could achieve ultra-wide frequency spectrum with narrow impulse, which has high range resolution for distinguishing targets with different dielectric characteristic in the back-scattering information. Pavement disengaging of air-coupled GPR system mainly focuses on range resolution and late-time ring. Generally, the frequency band was operated from 1 to 3 GHz, and the detection range was less than 0.5 meters. To achieve better performance, the taper line of horn antenna has been researched including linear, exponential, half-ellipse, etc. [13]. The plate TEM horn antenna was generally applied in the air-coupled GPR for its characteristic of ultra-wideband and easy fabrication. Foam-absorber loading could be easily fixed on the surface of horn arms and decrease the reflection from taper line with the cost of radiation efficiency [17]. Furthermore, it could decrease coupled between transmit (T) and receive (R) antenna. An dielectric wedge TEM horn antenna was developed with compact size and low-time ring [18]. It could not only improve isolation degree between T and R antenna, but also ensure the high fidelity. However, dielectric wedge antenna may have high cost and weight. In this paper, a modified TEM horn antenna with microstrip-type transmission is proposed. Design theory and the geometry of the antenna are briefly described in Section 2, and antenna characteristic is analyzed as well. In addition, the antenna integrated with radar receiver and transmitter is constructed and measured.

Received 5 May 2018, Accepted 16 October 2018, Scheduled 8 April 2019

* Corresponding author: Youcheng Wang (wangyoucheng99@163.com).

¹ Science and Technology on Complex System Control and Intelligent Agent Cooperation Laboratory, Beijing Electro-Mechanical Engineering Institute, Beijing, China. ² Key Laboratory of Electromagnetic Radiation and Sensing Technology, Chinese Academy of Sciences, Beijing, China.

2. ANTENNA DESIGN AND DISCUSSION

TEM horn has been considered as a transformer that transforms input impedance to free space in which the wave impedance is 120π ohm. According to [17], the transmission line wave field required currents on the antenna conductor and was not the same as a spherical wave in free space. It means that 120π may not be the optimum value. Better performance of air-couple antenna was achieved when the impedance of horn aperture was 180 ohm in [19]. To achieve maximum gain for a given aperture, the taper should be long enough so that the phase of antenna was approximately constant at the cross-section of aperture. However, air-coupled radar system integrated with a limited size of horn antenna was operated in a box at the end of the car for sensing pavement subsurface. According to [19], the reflection coefficient of the horn antenna can be mainly decomposed into three components: port reflection, taper reflection, and aperture reflection. The mismatch in the feeding structure was responsible for the port reflection, which may be minimized with a transmission of 50 ohm unbalance type. The aperture reflections may be reduced by optimizing aperture structure. The taper reflections seem to be ascribed to the nonuniform geometry of the taper along with the throat to the horn aperture, which was responsible for the impedance bandwidth. Various methods for specifying the gradual change of impedance in cross-section along the taper line have been studied, including exponential, linear, half-ellipse line, optimum taper, etc. In this paper, a quasi-optimum taper was employed [20], which was found to achieve the lowest reflection with limited length. The cross-section dimension of the plate horn was calculated by conformal-mapping approximation [21]. Transmitting and receiving (T/R) antennas were operated side by side with a distance in air-coupled GPR system. Suitable isolation degree of radar receiver was helpful to the radar receiver that could detect near-field target's weak signal in the dynamic range. Dielectric-filled TEM horn could achieve compact size and improve isolation degree with high cost for manufacturing [18]. Foam-absorber loading method was applied to decrease coupling between T and R antennas. The impedance matching was critical to the bandwidth as well; therefore, a compact microstrip-type balun was designed for matching the antenna and radar port [20]. The size of radar system was given for engineering application. The length of antenna should be beyond the request. There are two steps for horn antenna design which contains two transformers. Firstly, the horn antenna could be regard as a transformer which transforms balance impedance of horn throat to balance impedance of horn aperture. The other transformer transforms the coaxial feed of unbalance impedance at 50 ohm to the horn throat at balance impedance. Then, impedance of horn throat at 65 ohm was accepted in the optimized antenna. The question was how to match the balance impedance at 65 ohm to the unbalance impedance at 50 ohm. A 'near'-optimum taper design was accepted which avoided the impedance steps and yielded tapers of fractional part longer in taper length [22]. After the theory dimension of balun was calculated, the key parameters were optimized by particle swarm algorithm. The geometry of antennas was shown in Fig. 1, in which L_a is the axial length of the antenna, W_a the width of the taper arm, and H_{sub} the height of both the substrate and the antenna. Z_a is the impedance at the cross-section along the quasi-optimum taper arms with a given reflection level. The impedance across the horn aperture was set as 200 ohm. Fig. 2 illustrates the width and height of cross-section along the horn antenna. The height of antenna throat was approximately one lambda of upper frequency in free space. When the impedance along the taper was defined, the width of horn antenna arms can be calculated by conformal-mapping approximation. The geometry dimension is shown in Table 1. In Fig. 3, simulated current distribution of the horn antenna without resistive loading is presented at different frequencies. It is obvious that the currents flowed from horn antenna throat to the antenna aperture. The surface currents of arms mostly concentrated on the edge of the horn plate. With the frequency increased, the current tended to the center of antenna arms. The cross-polarization currents in high frequency would lead to the split of main lobe which affected the performance of antenna direction. That foam-absorber loaded at the back of horn arm can absorb the remnant currents and diffracted wave around the edge of arms. However, foam-absorber loading would reduce the radiation efficiency with the cost of waveform amplitude. To study the time-domain characteristic, near-field radiating waveform of the antenna without resistive-loaded is shown in Fig. 4. The simulated parameters were set as follows. Four probes were placed in a circle around E -plate of the antenna with a step of 30 degrees. One probe was implemented at the back of horn antenna, and the radius of circle was 400 mm. The excited source signal was a Gaussian pulse, whose amplitude was 1 V. Fig. 4 illustrates that simulated non-normalized waveform of E -plate varies obviously as the angle

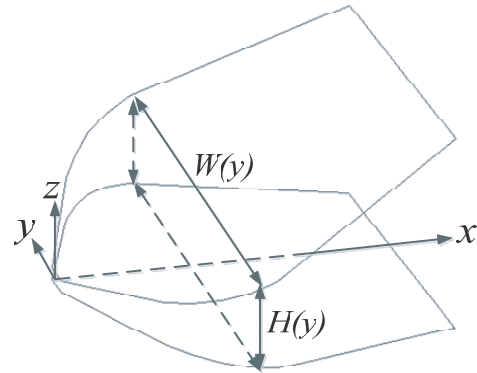
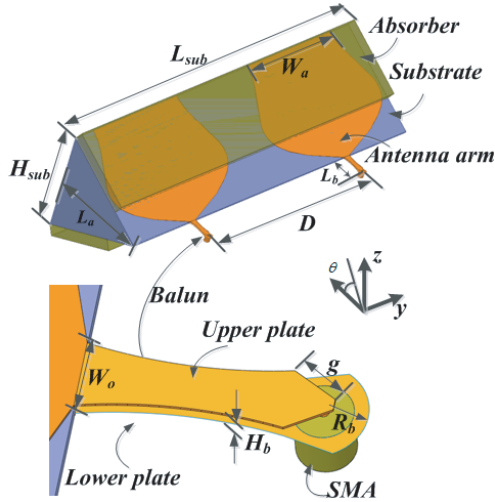


Figure 1. The geometry structure dimension of the antenna as follow: $D = 350$ mm, $H_b = 2$ mm, $L_b = 39.5$ mm, $R_b = 8.85$ mm, $g = 8.7$ mm.

Figure 2. The structure of the proposed antenna.

Table 1. Dimension of TEM horn antennas.

L_a (mm)	W_a (mm)	H_{sub} (mm)	Z_a (ohm)	L_a (mm)	W_a (mm)	H_{sub} (mm)	Z_a (ohm)
0.0	12.0	2.0	50.0	99.0	250.0	106.5	103.2
9.0	66.3	11.5	51.7	108.0	242.2	116.0	112.2
18.0	115.1	21.0	53.9	117.0	233.0	125.5	121.5
27.0	157.3	30.5	56.6	126.0	223.3	135.0	131.1
36.0	192.2	40.0	60.0	135.0	214.2	144.5	140.7
45.0	219.6	49.5	64.0	144.0	206.0	154.0	150.1
54.0	239.3	59.0	68.6	153.0	199.0	163.5	158.9
63.0	252.0	68.5	74.1	162.0	193.7	173.0	167.0
72.0	258.5	78.0	80.2	171.0	190.1	182.5	174.1
81.0	259.6	87.5	87.2	180.0	188.6	192.0	180.0
90.0	256.5	97.0	94.9				

increases. When the probe was placed at the back of the antenna, the amplitude of waveform decreased quickly, suggesting that the back radiation of the horn antenna was small. The maximum radiation waveform occurred in the front of the aperture. The late-time ripple was also obvious in near-field region. However, foam-absorber loading decreased late-time ring of time domain waveform.

3. MEASUREMENTS AND EXPERIMENTS

One pair of antennas was manufactured and shown in Fig. 5. The construed antenna contained two metal plates which were fixed by foams. The Cumming company absorber LF77 was placed on the horn antenna’s surface. Its characteristic was measured by Agilent N5242A after calibration. The measured results of both absorber loading and no loading agreed well with the simulated results in Fig. 6. It was obvious that the antenna with absorber loading achieved a lower return loss than the horn antenna without loading. Some discrepancies have happened at several tuned frequencies between measured and

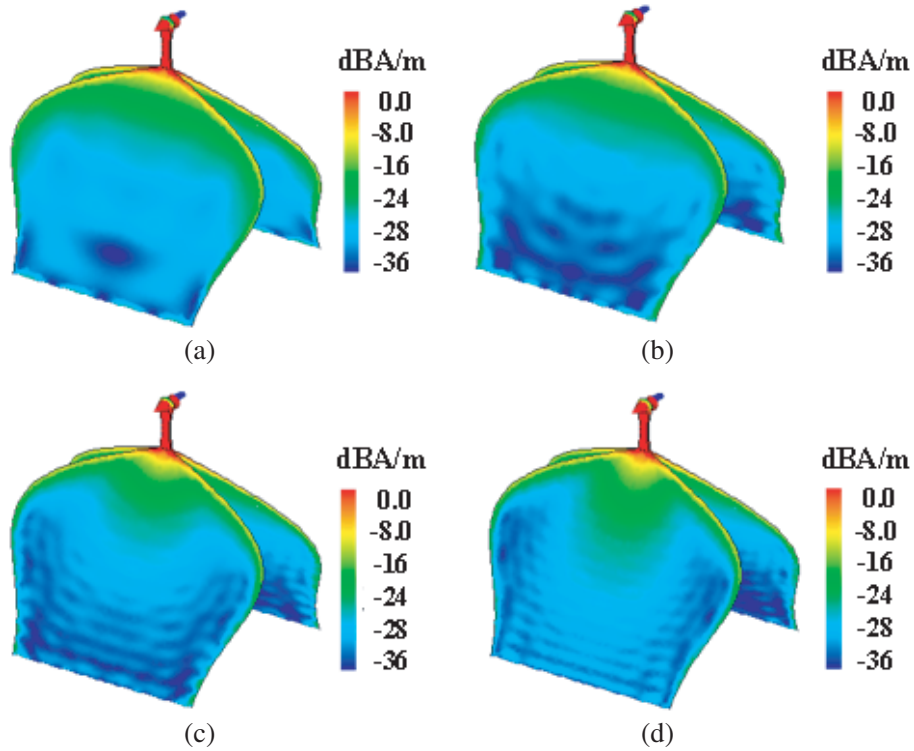


Figure 3. Simulated current distribution of the horn antenna at: (a) 2 GHz; (b) 6 GHz; (c) 10 GHz; (d) 12 GHz.

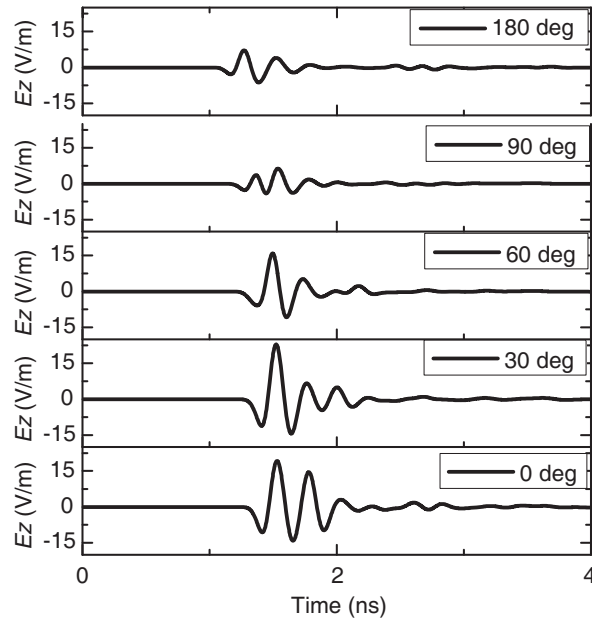


Figure 4. Simulated non-normalized waveform of E -plate (xoz plate) without resistive-loaded.

simulated return losses, probably because the performance of impedance matching was easily affected by the manufacture deviation of balun. The measured result showed that the bandwidth of the antenna was from 0.5 to 14 GHz with the return loss less than -10 dB. There was a tendency that the antenna has upper bandwidth with return loss less than -12 dB at 14 GHz. Measured radiation patterns of both

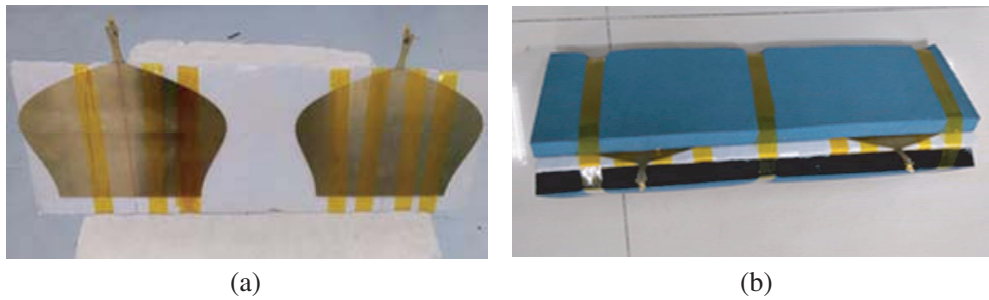


Figure 5. The manufactured antenna, (a) without foam-absorber loaded; (b) with foam-absorber loaded).

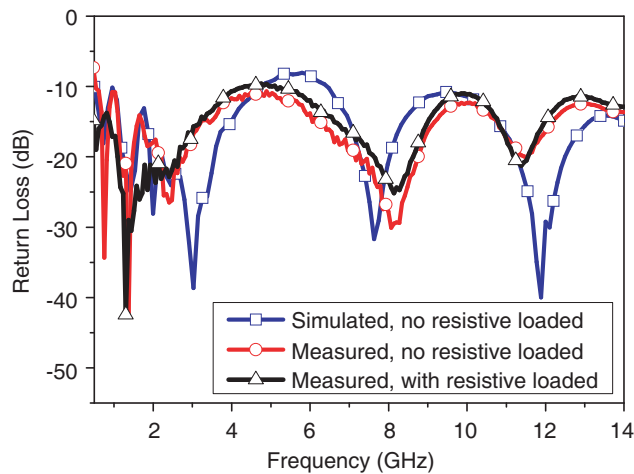


Figure 6. Comparison measured and simulated S parameters.

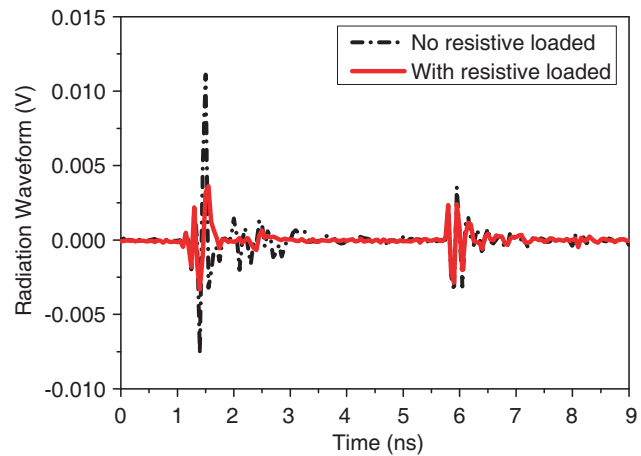


Figure 7. Comparison measured waveform with or no foam-absorber load.

E -plane and H -plane are shown in Fig. 8. There was only one dominant lobe and back radiation which was small. The side lobe was obvious with increased frequency. Performance of the H -plane pattern was leaning at 6 GHz because the T/R antennas operated together side by side. The center frequency of air-coupled GPR system was operated at 2 GHz, and the proposed TEM horn antenna had good radiation pattern of E -plane.

A pair of antennas was implemented 0.5 meters above ground, and the measured waveforms of the antennas with or without resistive loading are shown in Fig. 7. It is obvious that the reflection from ground appeared at time of 5.8 ns. After resistive loading, the peak of directive waveform was reduced approximately 3 dB, and the late-time ring was also decreased. To verify the antenna design, a pavement layer detecting experiment was applied. The antennas were integrated with impulse radar on vehicle-mounted platform. The air-coupled GPR system was constructed over the ground with a height of 0.5 meters, in which transmitter and receiver antennas were packed in a box mounted on a wood frame that was fixed on the end of a car. To verify performance of the antenna, a pavement layer detecting experiments was applied. A stationary test was first conducted to measure the reflection wave by collecting GPR data over a large flat copper plate placed on the pavement surface. The radar image, after radar data were processed as procedure [5], is shown in Fig. 9, which displays high image resolution. The radar image contained a number of A-scan data, which can be processed by the approach as in [23]. In Fig. 10, a number of layers can be clearly distinguished, and trace correlation experiments results showed that the layers appeared approximately on the time including 0.6 ns, 1.2 ns, and 2.5 ns. We can calculate the layer thickness of pavement after its dielectric constant is measured. The radar image experiments results indicated that characteristics of the antenna met the requirements of sensing pavement subsurface.

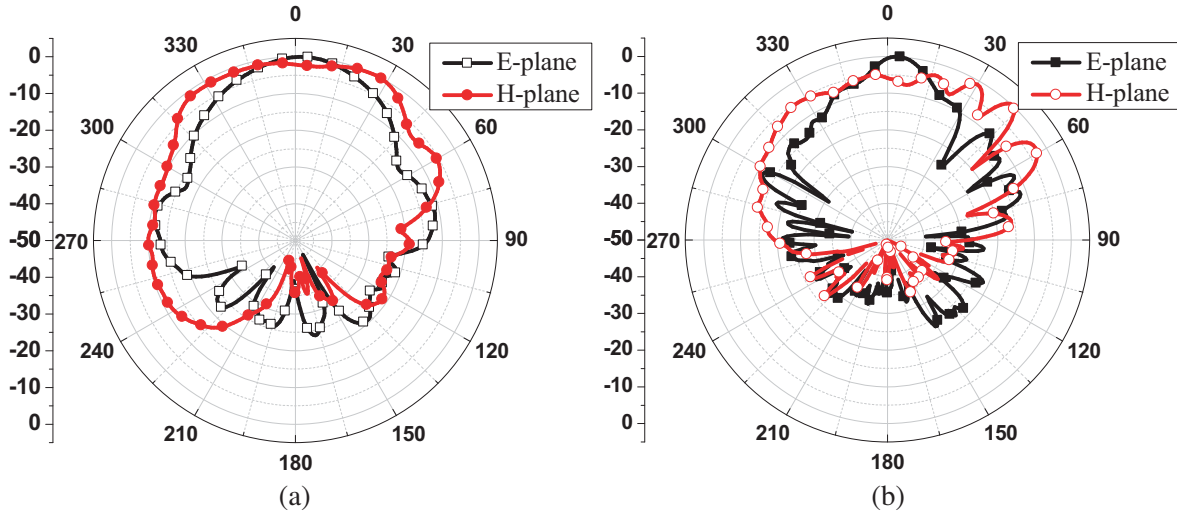


Figure 8. Measured radiation pattern (T/R) at: (a) 2 GHz; (b) 6 GHz.

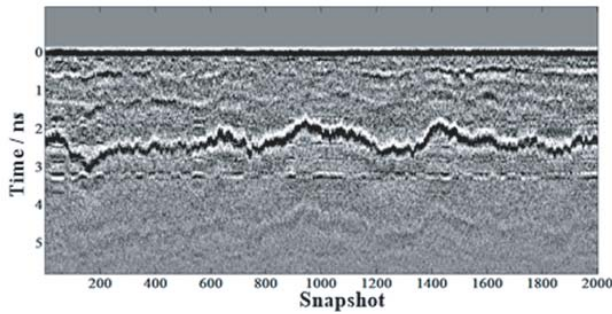


Figure 9. Experiment results for sensing pavement subsurface.

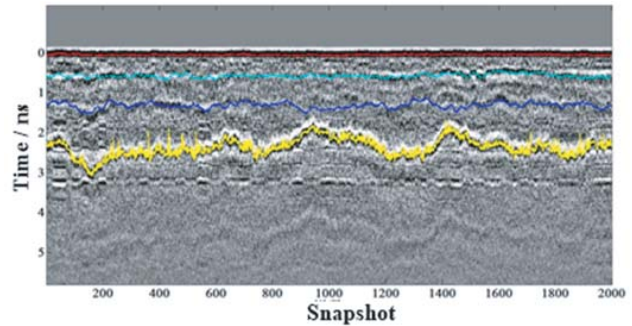


Figure 10. Trace correlation experiments results.

4. CONCLUSION

We have presented a resistive-loaded TEM horn antenna designed to apply in an air-coupled GPR system. The investigated parameters of the antenna were the taper arm and feeding structure. The quasi-optimum taper was employed to construct the horn arms. An unbalance-to-balance transformer was designed together with the antenna. To validate the design, an integrated T/R antenna was constructed. We have measured the frequency and time-domain characteristics of the antenna. The results showed that the antenna showed an ultra-wide bandwidth and outstanding waveform performance. The radar experiment showed that characteristic of the antenna could be applied in the pavement layer detection.

ACKNOWLEDGMENT

This work has been supported by the National Natural Science Foundation of China (Number: 61701465). The author would like to thank Prof. Guangyou Fang, Chinese Academy of Sciences, China. The same thanks to anonymous peer reviewers here.

REFERENCES

1. Loizos, A. and C. Plati, "Accuracy of ground penetrating radar horn-antenna technique for sensing pavement subsurface," *IEEE Sensors Journal*, Vol. 7, 842–850, 2007.

2. Willett, D. A., K. C. Mahboub, and B. Rister, "Accuracy of ground-penetrating radar for pavement-layer thickness analysis," *Journal of Transportation Engineering*, Vol. 132, 96–103, 2006.
3. Loizos, A. and C. Plati, "Accuracy of pavement thicknesses estimation using different ground penetrating radar analysis approaches," *NDT & E International*, Vol. 40, 147–157, 2007.
4. Han, J. and C. Nguyen, "Development of a tunable multiband UWB radar sensor and its applications to subsurface sensing," *IEEE Sensors Journal*, Vol. 7, 51–58, 2007.
5. Al-Qadi, I. and S. Lahouar, "Measuring layer thicknesses with GPR — Theory to practice," *Construction and Building Materials*, Vol. 19, 763–772, 2005.
6. Saarenketo, T. and T. Scullion, "Road evaluation with ground penetrating radar," *Journal of Applied Geophysics*, Vol. 43, 119–138, 2000.
7. Dérobert, X., J. Iaquina, G. Klysz, and J. P. Balayssac, "Use of capacitive and GPR techniques for the non-destructive evaluation of cover concrete," *Ndt & E International*, Vol. 41, 44–52, 2008.
8. Shao, J., G. Fang, Y. Ji, and H. Yin, "Semicircular slot-tuned planar half-ellipse antenna with a shallow vee-cavity in vital sign detection," *IEEE Journal of Selected Topics in Applied Earth Observations and Remote Sensing*, Vol. 7, 767–774, 2014.
9. Seyfried, D., R. Jansen, and J. Schoebel, "Shielded loaded bowtie antenna incorporating the presence of paving structure for improved GPR pipe detection," *Journal of Applied Geophysics*, Vol. 111, 289–298, 2014.
10. Bai, J., S. Shi, and D. W. Prather, "Modified compact antipodal vivaldi antenna for 4–50-GHz UWB application," *IEEE Transactions on Microwave Theory and Techniques*, Vol. 59, 1051–1057, 2011.
11. Ma, K., Z. Zhao, J. Wu, S. M. Ellis, and Z.-P. Nie, "A printed vivaldi antenna with improved radiation patterns by using two pairs of eye-shaped slots for UWB applications," *Progress In Electromagnetics Research*, Vol. 148, 63–71, 2014.
12. Uduwawala, D., M. Norgren, P. Fuks, and A. W. Gunawardena, "A deep parametric study of resistor-loaded bow-tie antennas for ground-penetrating radar applications using FDTD," *IEEE Transactions on Geoscience and Remote Sensing*, Vol. 42, 732–742, 2004.
13. Campbell, M. A., O. Michal, and E. C. Fear, "TEM horn antenna for near-field microwave imaging," *Microwave and Optical Technology Letters*, Vol. 52, 1164–1170, 2010.
14. Shlager, K. L., G. S. Smith, and J. G. Maloney, "TEM horn antenna for pulse radiation: An improved design," *Microwave and Optical Technology Letters*, Vol. 12, 86–90, 1996.
15. Shao, J., G. Fang, J. Fan, Y. C. Ji, and H. Yin, "TEM horn antenna loaded with absorbing material for GPR applications," *IEEE Antennas and Wireless Propagation Letters*, Vol. 13, 523–527, 2014.
16. Dehdasht-Heydari, R., H. R. Hassani, and A. R. R. Mallahzadeh, "Quad ridged horn antenna for UWB applications," *Progress In Electromagnetics Research*, Vol. 79, 23–38, 2008.
17. Theodorou, E. A., M. R. Gorman, P. R. Rigg, and F. N. Kong, "Broadband pulse-optimised antenna," *IEE Proceedings H, Microwaves Optics and Antennas*, Vol. 128, 124–130, 1981.
18. Yarovoy, A. G., A. D. Schukin, I. V. Kaploun, and L. P. Ligthart, "The dielectric wedge antenna," *IEEE Transactions on Antennas and Propagation*, Vol. 50, 1460–1472, 2002.
19. Tan, A.-C., K. Jhamb, and K. Rambabu, "Design of transverse electromagnetic horn for concrete penetrating ultrawideband radar," *IEEE Transactions on Antennas and Propagation*, Vol. 60, 1736–1743, 2012.
20. Hecken, R. P., "A near-optimum matching section without discontinuities," *IEEE Transactions on Microwave Theory and Techniques*, Vol. 20, 734–739, 1972.
21. Wheeler, H. A., "Transmission-line properties of parallel wide strips by a conformal-mapping approximation," *IEEE Transactions on Microwave Theory and Techniques*, Vol. 12, 280–289, 1964.
22. Hecken, R. P., "A near-optimum matching section without discontinuities," *IEEE Transactions on Microwave Theory and Techniques*, Vol. 20, 734–739, 1972.
23. Daniels, D. J., *Ground Penetrating Radar*, Chapter 2, John Wiley & Sons, Inc., 2005.